CH$_4$/CO$_2$ separation from biogas stream using porous hydrophobic ceramic hollow fiber membrane contactors

Hong Joo Lee, Min Kwang Kim, Seung Hwan Lee, and Jung Hoon Park[†]

Department of Chemical and Biochemical Engineering, Dongguk University, Wonheung-gwan F619,
30, Pildong-ro 1gil, Jung-gu, Seoul 04620, Korea

Abstract−Experiments were performed to separate CO$_2$ from biogas using a ceramic hollow fiber membrane contactor (HFMC). CH$_4$/CO$_2$ mixed gas (34.5% CO$_2$, CH$_4$ balance) and monoethanolamine (MEA) were used. The influence of operating conditions, such as the gas flow rate, liquid flow rate, L/G ratio, CO$_2$ partial pressure, and module type, on the CO$_2$ removal efficiency and CO$_2$ absorption flux was evaluated. As the gas flow rate increased, the CO$_2$ removal efficiency decreased, while the CO$_2$ absorption flux increased. The maximum CO$_2$ removal efficiency was 96% at a gas flow rate of 0.1 Nm^3 h^{-1} while the maximum CO$_2$ absorption flux was 7.5×10^{-3} mol·m^{-2}·s^{-1} at a gas flow rate of 1 Nm^3 h^{-1}. Moreover, the CO$_2$ absorption flux and CO$_2$ removal efficiency could be increased by more than 20% using the high-flux module.

Keywords: Membrane Contactor, Hydrophobic Ceramic Membrane, CO$_2$ Separation, Biogas Purification

INTRODUCTION

Alternative energy sources are being actively developed worldwide to prepare for rising crude oil prices and to secure stable energy source supplies [1]. According to international environmental regulations and greenhouse gas reduction obligations enacted because of global warming, waste recycling, such as obtaining solid fuels from combustible wastes and biogas from organic wastes, has emerged as one potential means to reduce greenhouse gases [2]. CH$_4$, a main component of waste energy, is classified as one of the six major greenhouse gases; its global warming potential (GWP) is 21-times higher than that of CO$_2$, another major greenhouse gas [3]. Greenhouse gas reduction and renewable energy source security can be achieved through waste recycling [4]. Because the recycling of CH$_4$ as fuel can utilize existing natural gas infrastructures, CH$_4$ has greater potential short-term applicability than other renewable fuels [5].

Organic waste resources, such as food waste, leachates, sewage, wastewater sludge, and livestock manure, are converted into biogas through the anaerobic digestion process [6]. The components and compositions of biogas vary depending on the base material type of the source and the applied anaerobic digestion method. Biogas generally includes CH$_4$ (53-70%), CO$_2$ (30-47%), N$_2$O, H$_2$S, NH$_3$, H$_2$, N$_2$, and CO and requires purification processing before use as vehicle fuel or mixture with natural gas [7]. The CO$_2$ included in biogas may decrease its heating value and cause pipe corrosion [8]. Moreover, CO$_2$ is the best-known greenhouse gas [9]; therefore, technology to capture CO$_2$ from biogas must be developed to secure energy sources and to efficiently reduce greenhouse gas emissions [10].

Commercialized biogas purification technologies include water scrubbing, chemical absorption, pressure swing adsorption (PSA), membrane processing, and cryogenics. Water scrubbing requires high equipment costs and operational energy consumption because of its high operation pressures. To reduce the equipment scale, an efficient absorption column must be developed [11]. Chemical absorption operates at low pressure but generates wastewater and requires the development of high-efficiency absorbents and production processes because of absorbent deterioration [12]. PSA requires the development of high-performance adsorbents and hybrid processing because of its low selectivity for CH$_4$ and CO$_2$ and severe impurity contamination [13]. Membranes require development to overcome technical limitations such as the vulnerability of polymer membrane materials to sulfur compounds and low selectivity [14]. Cryogenics technology separates CH$_4$ and CO$_2$ using vapor pressure differences and requires high-cost equipment and significant energy consumption [15].

In membrane contactor technology, gas-liquid contact is achieved at the boundary of a hydrophobic porous membrane [16]. A mixed gas is contacted by a liquid-form absorbent that separates the mixed gas by selectively absorbing the high-solubility gas component [17]. The membrane contactor enables the construction of a simpler process compared to the conventional adsorption and membrane methods because it permits simultaneous removal of various impurities and CO$_2$ [18]. It is also a high-efficiency integrated purification technology with the benefits of small-sized equipment, easy scalability, and low installation and operation costs [19]. Most biogas sources are small- or medium-sized and geographically scattered. Because of these characteristics, the size, operation cost, and environmental friendliness of the pretreatment plant must be considered. The membrane contactor fulfills these requirements and is expected to show suitability for biogas purification [20].

[†]To whom correspondence should be addressed.
E-mail: pjhoon@dongguk.edu

Studies on the membrane contactor have used porous polymer hollow fiber membranes [21]. However, such polymer membranes experience geometric deformation due to the swelling of the absorption liquid, which sharply decreases the CO$_2$ absorption efficiency [22]. Therefore, membrane contactors using ceramic materials, which are more chemically and thermally stable than polymers, have been studied recently [23]. In our previous study, we developed a ceramic hollow fiber membrane contactor (HFMC) module capable of capturing CO$_2$ from mixed gas (N$_2$ balance) with a CO$_2$ concentration of around 15% [24]. Yu et al. [25] also conducted experiments to separate CO$_2$ from mixed gas with a 12.5% CO$_2$ concentration in N$_2$ using a single ceramic tubular membrane contactor and a monoethanolamine (MEA) absorbent.

Previous studies on ceramic membrane contactors have focused on CO$_2$ capture from power plant flue gases. Studies on the separation performance of ceramic membrane contactors in gas and fluid flows with high CO$_2$ concentrations (>30%), such as biogas, have not yet been reported. In this study, the separation process of CH$_4$/CO$_2$ from biogas was investigated using a ceramic HFMC. The CO$_2$ absorption properties were evaluated according to the operating conditions, such as the gas flow rate, liquid flow rate, liquid-gas (L/G) ratio, and CO$_2$ concentration; the influence of the HFMC module type was also investigated. The experiment results reported here may be used as basic data to design ceramic HFMC processes for CH$_4$/CO$_2$ separation.

EXPERIMENTAL

1. Al$_2$O$_3$ HFMC Module Fabrication

Al$_2$O$_3$ with high chemical stability was selected as the HFMC membrane material and purchased as two powders with 0.5-μm particle size and purities of 99.0% and 99.9% (Kceracell, Korea). A spinning solution was prepared by stirring 60 wt% Al$_2$O$_3$, 33.5 wt% methyl-2-pyrrolidone (NMP, 99.5%, Samchun Pure Chemical Co., Ltd., Korea), 6 wt% polyethersulfone (PESf, Ultrason® E6020P, BASF, Germany), and 0.5 wt% polyvinylpyrrolidone (PVP, Sigma Aldrich, USA) for two days. The prepared dope solution and internal coagulant (water) were each transferred to a container and spun by injection into a concentric double-tube-type spinneret using N$_2$ gas and a syringe pump. The spun hollow fibers experienced phase inversion as they passed through the air-gap and external coagulant (water). The spun Al$_2$O$_3$ hollow fiber membrane was cut to certain lengths, cleaned with water for 24 h, and oven dried overnight at 100 °C. The membranes were then sintered in a box furnace at 1,300 °C. The sintered hollow fiber membrane was then subjected to hydrophobic coating using heptadecafluoro-1,1,2,2-tetrahydrodecyl trimethoxysilane (FAS, ≥98%, Sooyang Chemtec Co., Ltd., Korea).

The hydrophobic hollow fiber membrane was cut to 20-cm lengths, and 200 strands were inserted into the housing of each module with an 80-mm inner diameter. Both ends of each hollow fiber membrane were sealed with a sealant. Curing was then performed by injecting a certain amount of epoxy adhesive into each housing. When the epoxy was completely cured, it was cut to avoid clogging the hollow fiber membranes. At the other end, the hollow fiber membrane was fixed to the housing in the same manner to fabricate a module.

2. CH$_4$/CO$_2$ Separation Experiment using HFMC

To investigate the CO$_2$ absorption properties of the fabricated ceramic HFMC, the experimental setup shown in Fig. 1 was used.
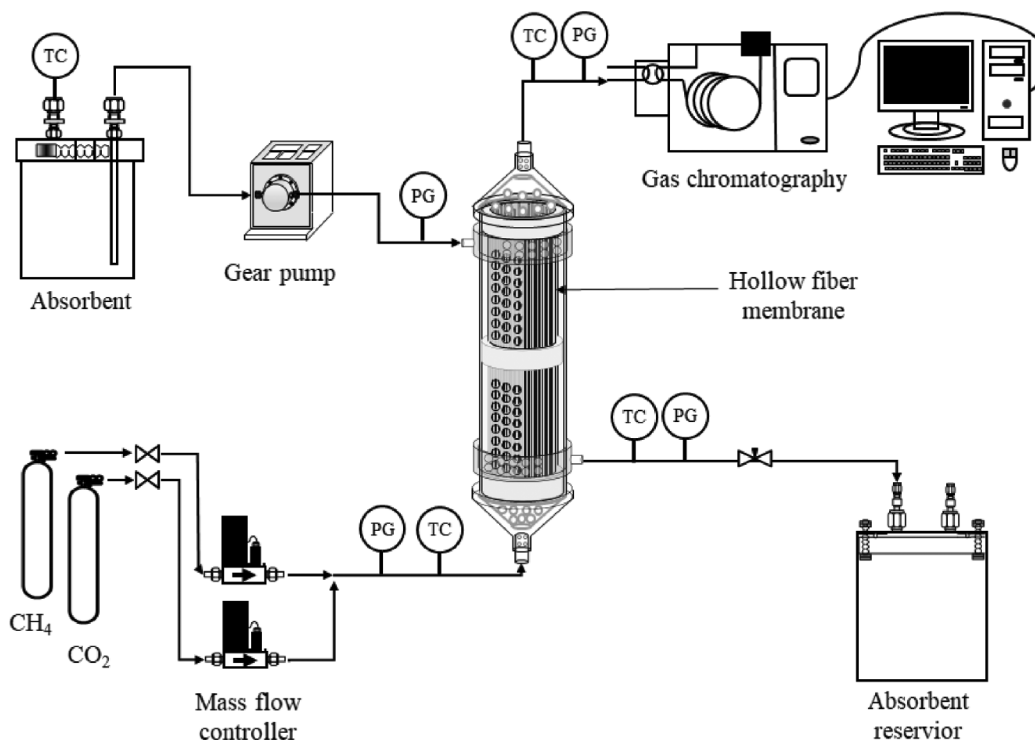

Fig. 1. Experimental setup of the ceramic HFMC for CH$_4$/CO$_2$ separation (TC: thermocouple, PG: pressure gauge).

Table 1. Operating conditions in the CH_4/CO_2 separation experiment using HFMC

Parameters		Value				
Gas flow rate ($Nm^3 h^{-1}$)		0.1	0.25	0.5	0.75	1
Liquid flow rate ($mL min^{-1}$)	L/G=5.63 (L Nm^{-3})	9.28	23.45	46.9	70.35	93.79
	L/G=7.03 (L Nm^{-3})	11.72	29.31	58.62	87.93	117.24
	L/G=9.38 (L Nm^{-3})	15.63	39.08	78.16	117.24	156.32

A CH_4 mixed gas containing 34.5% CO_2 is sent to the lumen side of the module using a mass flow controller (MFC, 5850E, Brooks, Japan), and a 30 wt% MEA (99.0%, Samchun Pure Chemical Co., Ltd., Korea) aqueous solution is simultaneously supplied to the shell side using a gear pump (REGLO-Z digital, Ismatec, USA). The mixed gas discharged from the membrane contactor absorption device is analyzed using gas chromatography (GC-TCD, iGC 7200, DS Science, Korea) to measure the CO_2 absorption amount and removal efficiency. Table 1 summarizes the membrane contactor operating conditions. The L/G ratio represents the ratio of the liquid flow rate to the gas flow rate.

RESULTS AND DISCUSSION

1. CO_2 Separation Performance of HFMC According to the Operating Conditions

Fig. 2 shows the CO_2 removal efficiency and CO_2 absorption flux results according to the gas flow rate at the L/G ratio of 5.63. As the gas flow rate is increased, the CO_2 removal efficiency tends to decrease, while the CO_2 absorption flux tends to increase. As the mass transfer resistance of the gas phase decreases according to the gas flow rate, the CO_2 absorption flux can increase [26]. However, as the gas flow rate is increased, the CO_2 removal efficiency is decreased because the residence time of the gas in the membrane contactor module is decreased, thus causing insufficient CO_2 absorption time [26]. The CO_2 removal efficiencies are 95.7% and 29.8% at the gas flow rates of 0.1 and 1 $Nm^3 h^{-1}$, respectively.

Fig. 3 shows the CO_2 absorption flux and CO_2 removal efficiency results of the membrane contactor according to varying L/G ratios,
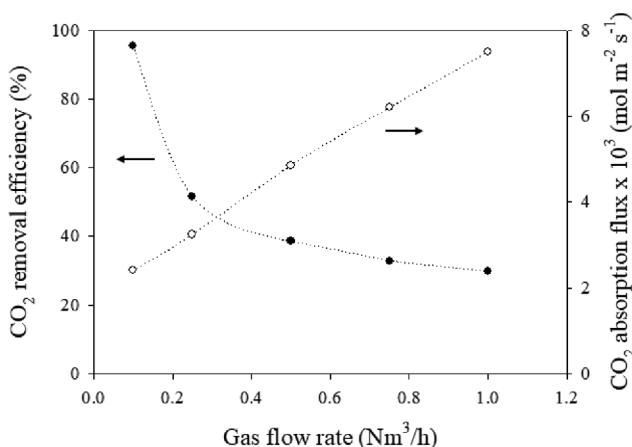
i.e., liquid flow rates. As shown, the influence of the liquid flow rate on the membrane contactor performance is not significant, but the performance shows slight increases with increases in the liquid flow rate. The MEA used in this study was a chemical absorbent with a high reaction rate with CO_2 and a loading ratio of (0.5 mol CO_2)/(1 mol MEA) [27]. A sufficient concentration gradient for absorbing CO_2 was maintained during the experiment. Therefore, the results of Fig. 2 and Fig. 3 confirm that the membrane contactor process using MEA is dominated by the mass transfer resistance of the gas phase [28].
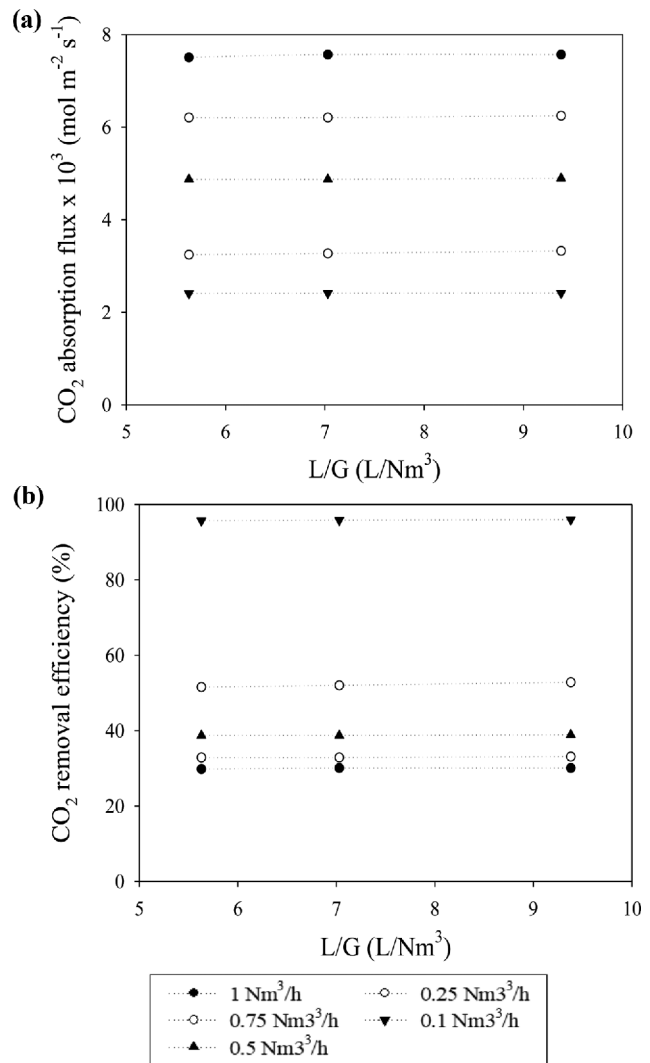

Fig. 3. (a) CO_2 absorption flux and (b) CO_2 removal efficiency according to the liquid flow rate.

Fig. 2. CO_2 removal efficiency and CO_2 absorption flux according to the gas flow rate.
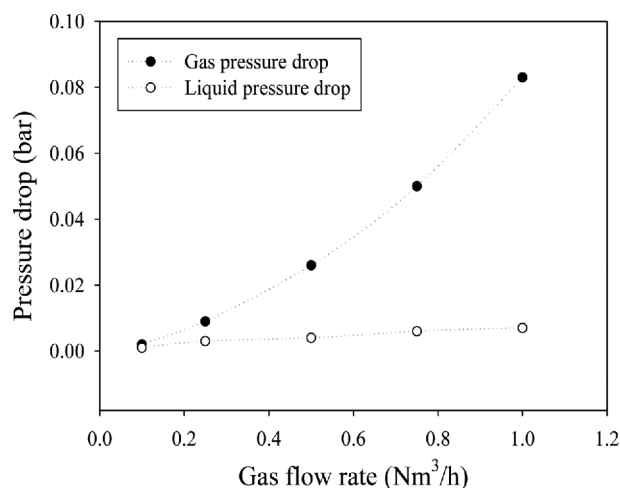
Fig. 4. Gas and liquid pressure drops according to the gas flow rate.

Fig. 4 shows the pressure drop according to the gas flow rate at the L/G ratio of 5.63. As the gas flow rate is increased, the gas pressure drop is increased while the liquid pressure drop remains almost constant. In addition, the liquid pressure drop is negligible compared to the gas pressure drop. Large gas pressure drops are known to increase the process operation cost by increasing the required pump power. The gas pressure drop in the conventional packed-column absorption process is known to be approximately ≤0.05 bar [29], and the pressure drops measured in the ceramic HFMC experiments are similar or lower. The membrane contactor process can therefore reduce the pressure drop while exhibiting high CO$_2$ absorption properties.

Fig. 5 shows the CO$_2$ absorption flux results of the membrane contactor according to the CO$_2$ concentration in the gas at the gas flow rate of 0.5 Nm^3 h^{-1} and the L/G ratio of 5.63. As the CO$_2$ concentration is increased, the CO$_2$ absorption flux increases. This may arise from the increase in the absorption driving force as the gas-phase CO$_2$ partial pressure is increased. At the CO$_2$ concentration
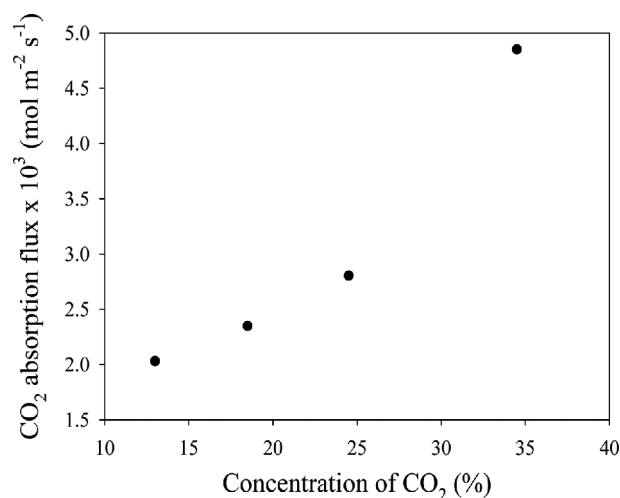

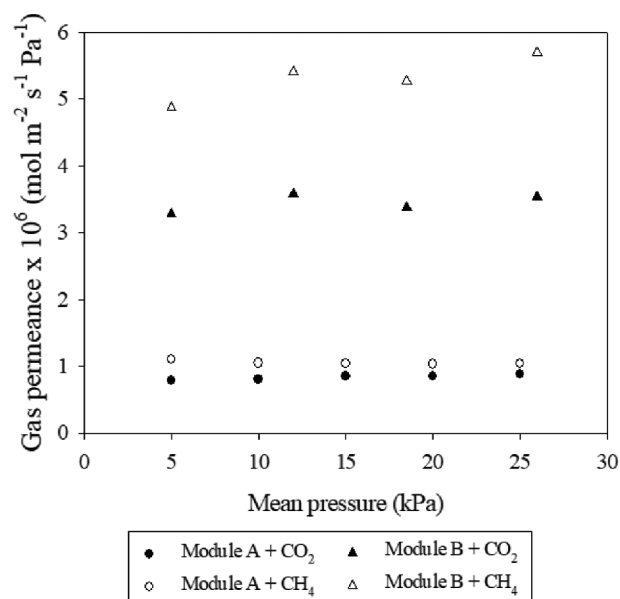Fig. 5. CO$_2$ absorption flux according to the CO$_2$ concentration in the mixed gas.

Fig. 6. Single-gas (CO$_2$ and CH$_4$) permeance according to the HFMC module types.

in the feed gas of 34.5% and 24.5%, the CO$_2$ concentration in the outlet gas is approximately 24.5% and 18.2%, respectively. Therefore, based on the results of Fig. 5, the CO$_2$ absorption performance can be roughly predicted for two modules connected in series. These results can be utilized as important basic data for the connection of unit modules in series or in parallel for process scale-up.

2. CO$_2$ Absorption Properties According to the Ceramic HFMC Module Types

Fig. 6 shows the single-gas permeance of the module types A and B. Modules A and B comprise the hollow fiber membranes prepared using Al$_2$O$_3$ powders with purities of 99.0% and 99.9%, respectively. Modules A and B have equal fiber numbers, packing densities, and membrane areas. The gas permeance of module B is higher than that of module A (Fig. 6). Impurities in the Al$_2$O$_3$ powders include SiO$_2$, MgO, Fe$_2$O$_3$, and Na$_2$O. These impurities are known to decrease the Al$_2$O$_3$ sintering temperature [30]. Therefore, it appears that the gas permeance of module A is lower because the greater impurity concentration hinders pore formation in the hollow fiber membranes. Moreover, the permeance of CH$_4$ is slightly higher than that of CO$_2$ in both modules A and B. The flow due to Knudsen diffusion is known to be inversely proportional to the square root of the molecular weight [31]. Because the molecular weight of CH$_4$ is smaller than that of CO$_2$, the results in Fig. 6 show agreement with the mechanism of Knudsen diffusion, which is dominant when the pore size of the hollow fiber membrane is <1×10^{-7} m [31].

The results in Fig. 7 confirm that module B with high gas permeance has higher CO$_2$ removal efficiency and CO$_2$ absorption flux than module A. Membranes with higher flux have lower membrane mass transfer resistance in the membrane contactor process [32]. Based on these results, the CH$_4$/CO$_2$ separation properties could be improved through controlling the pore structures of the hollow fiber membranes and module optimization.
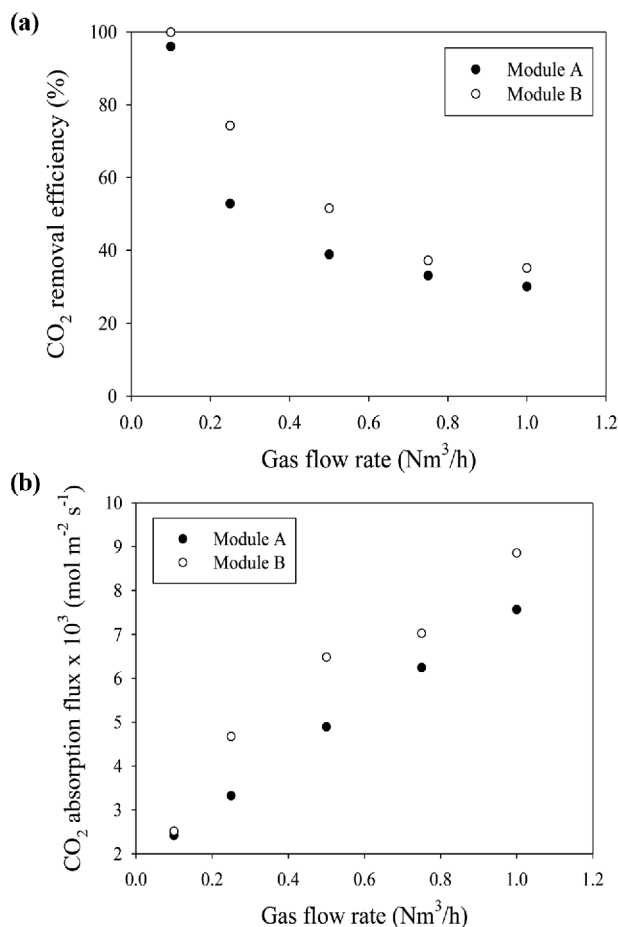
(a)

(b)

Fig. 7. (a) CO_2 removal efficiency and (b) CO_2 absorption flux according to the HFMC module types.

CONCLUSIONS

A chemical absorption process was developed using a ceramic HFMC to capture high-concentration CO_2 from a biogas flow. Ceramic HFMC modules were fabricated using the phase-inversion spinning method. The CO_2 absorption performance of the ceramic HFMC was evaluated according to the operating conditions, such as the gas flow rate, liquid flow rate, L/G ratio, and CO_2 partial pressure. The CO_2 removal efficiency decreased as the gas flow rate increased, and the influence of the liquid flow rate on the efficiency was not significant. The HFMC process using MEA as a chemical absorbent was dominated by the gas-phase mass transfer resistance. Moreover, the CO_2 separation performance was improved using a high-flux module with a higher-purity ceramic precursor. These experimental results are expected to be highly useful as basic data for the design of the ceramic HFMC process. The ceramic HFMC can replace the conventional packed absorption column or polymeric membrane contactor as a process with high potential utility in the biogas purification process.

ACKNOWLEDGEMENTS

REFERENCES

1. P. Lunghi, R. Bove and U. Desideri, *J. Power Sources*, **131**(1-2), 120 (2004).
2. A. Bandyopadhyay, *Clean Technol. Environ. Policy*, **13**(2), 269 (2011).
3. S. H. Yeon, B. K. Seo, Y. I. Park and G. H. Lee, *Korean Chem. Eng. Res.*, **39**(6), 709 (2001).
4. K. B. Hogan, J. S. Hoffman and A. M. Thompson, *Nature*, **354**, 181 (1991).
5. S. W. Lee, E. J. Kim, H. J. Lee and J. H. Park, *Korean Chem. Eng. Res.*, **56**(3), 297 (2018).
6. R. Bove and P. Lunghi, *Energy Convers. Manage.*, **47**(11-12), 1391 (2006).
7. Y. C. Park, J. S. Lee, J. H. Moon, B. M. Min, D. M. Shim and H. J. Sung, *Korean J. Chem. Eng.*, **34**(3), 921 (2017).
8. S. Atchariyawut, R. Jiraratananon and R. Wang, *J. Membr. Sci.*, **304**(1-2), 163 (2007).
9. L. Cong, Z. Ying, X. Yongqing, D. Haoran, Z. Chuguang, Q. Changlei and F. Bo, *Korean J. Chem. Eng.*, **32**(5), 934 (2015).
10. S. Atchariyawut, R. Jiraratananon and R. Wang, *Sep. Purif. Technol.*, **63**(1), 15 (2008).
11. J. Läntelä, S. Rasi, J. Lehtinen and J. Rintala, *Appl. Energy*, **92**, 307 (2012).
12. S. Rasi, J. Läntelä and J. Rintala, *Fuel*, **115**, 539 (2014).
13. S. Cavenati, C. A. Grande and A. E. Rodrigues, *Energy Fuels*, **19**(6), 2545 (2005).
14. H. J. Kim and S. I. Hong, *Korean J. Chem. Eng.*, **14**(5), 382 (1997).
15. S. Cavenati, C. A. Grande and A. E. Rodrigues, *Chem. Eng. Sci.*, **61**(12), 3893 (2006).
16. D. Jeong, M. Yun, J. Oh, I. Yum and Y. Lee, *Korean J. Chem. Eng.*, **27**(3), 939 (2010).
17. N. Nabian, A. A. Ghoreyshi, A. Rahimpour and M. Shakeri, *Korean J. Chem. Eng.*, **32**(11), 2204 (2015).
18. N. Ghasem, M. Al-Marzouqi and A. Duidar, *Sep. Purif. Technol.*, **98**, 174 (2012).
19. H. J. Lee, Y. G. Park, M. K. Kim, S. H. Lee and J. H. Park, *Sep. Purif. Technol.*, **220**, 189 (2019).
20. A. Mansourizadeh, A. F. Ismail, M. S. Abdullah and B. C. Ng, *J. Membr. Sci.*, **355**(1-2), 200 (2010).
21. G. Bakeri, M. Rezaei-DashtArzhandi, A. F. Ismail, T. Matsuura, M. S. Abdullah and B. C. Ng, *Korean J. Chem. Eng.*, **34**, 160 (2017).
22. E. Magnone, H. J. Lee, J. W. Che and J. H. Park, *J. Ind. Eng. Chem.*, **42**, 19 (2016).
23. H. J. Lee, E. Magnone and J. H. Park, *J. Membr. Sci.*, **494**, 143 (2015).
24. H. J. Lee and J. H. Park, *J. Membr. Sci.*, **518**, 79 (2016).
25. X. Yu, L. An, J. Yang, S.-T. Tu and J. Yan, *J. Membr. Sci.*, **496**, 1 (2015).
26. Y. Lv, X. Yu, S. T. Tu, J. Yan and E. Dahlquist, *Appl. Energy*, **97**, 283 (2012).
27. Y. E. Kim, J. H. Choi, S. H. Yun, S. C. Nam and Y. I. Yoon, *Korean J. Chem. Eng.*, **33**(12), 3465 (2016).
28. H. J. Lee, M. Binns, S. J. Park, E. Magnone and J. H. Park, *Korean J.*

Chem. Eng., **36**(10), 1669 (2019).
29. A. Zakeri, A. Einbu and H. F. Svendsen, *Chem. Eng. Sci.*, **73**, 285 (2012).
30. Y. Kim, S. Kim. J. Kim. Y. Cho, H. Park, P. Lee, Y. Park, H. Park

and S. Nam, *Membr. J.*, **28**, 21 (2018).
31. S. Boributh, S. Assabumrungrat, N. Laosiripojana and R. Jiraratananon, *J. Membr. Sci.*, **380**, 21 (2011).
32. J. Li and B. Chen, *Sep. Purif. Technol.*, **41**, 109 (2005).